J. Chem. Sci. (2020)132:15
https://doi.org/10.1007/s12039-019-1700-z

REGULAR ARTICLE

A hydrogel based on dialdehyde carboxymethyl cellulose–gelatin and its utilization as a bio adsorbent

SAPNA SETHI[a,*], BALBIR SINGH KAITH[b], MANDEEP KAUR[a], NEERAJ SHARMA[a] and SADHIKA KHULLAR[b,*]

[a]Department of Chemistry, DAV University, Jalandhar 144 012, Punjab, India
[b]Department of Chemistry, Dr. B.R. Ambedkar National Institute of Technology, Jalandhar 144 011, Punjab, India
E-mail: sapna10062@davuniversity.org; khullars@nitj.ac.in

MS received 10 May 2019; revised 23 August 2019; accepted 30 August 2019

Abstract. In the present study, the dialdehyde carboxymethyl cellulose (DCMC) was cross-linked covalently to gelatin *via* the Schiff base reaction to form a three-dimensional hydrogel (DCMC-cl-G). The crosslinking degree of DCMC and gelatin was estimated to be 50.31 ± 2.65. The maximum swelling capacity of the hydrogel in aqueous medium was around 74 g/g at pH 10.0 and 37 °C with equilibrium swelling attained in three hours and the compressive strength of the hydrogel was found to be 55 ± 0.76 kPa at 60% strain. The biodegradation studies confirmed 82.67% degradation of the hydrogel sample within a period of twelve weeks. Further, the hydrogel was evaluated as a bio adsorbent for the removal of hazardous dyes, namely Rhodamine B (RhB) and Methyl Violet (MV) from water due to its decent swelling capacity and good mechanical strength. The maximum percentage of RhB and MV removed from the respective dye solutions using DCMC-cl-G hydrogel was 96.5% and 90% at pH 6.0, respectively. Both dyes followed Langmuir adsorption isotherm, which considers monolayer adsorption of adsorbate over adsorbent, with a pseudo-second-order kinetic model.

Keywords. Eco-friendly; biodegradation; cross-linked; dye removal; natural polysaccharides.

1. Introduction

Water pollution by various industrial effluents such as dyes, heavy metal ions, and other organic contaminants such as pesticides, drugs, etc., has increased leaving an intimidating remark on the environment.[1] Out of these effluents, the waste from the dye industry contributes enormously to the water quality and thus makes it unfit for drinking. The world is suffering from severe scarcity of water and thus protecting drinking water is the need of the hour. Therefore, the scientific and general community should contribute immensely to protecting it. There are many techniques such as membrane filtration, coagulation, ozone treatment, photocatalytic degradation, ion exchange, biological treatment, etc., which are employed to remove dyes from wastewater. Out of all these methods, adsorption is an easy, practical, and cost-effective method.[2] Thus the synthesis of materials with high adsorbing quality is essential to efficiently adsorb dyes from water.

Hydrogels are hydrophilic in nature with three-dimensional structures which can retain water in it, showing its good absorbing capacity. Polymeric hydrogels of natural polysaccharides, such as starch, gelatin, chitosan, sodium alginate, gums, polypeptides, agar, etc., and carboxymethyl cellulose (CMC) have been receiving considerable attention due to their promising wide range of applications in the fields of biomedical, pharmacy, nanotechnology, electrochemical capacitor, water and soil treatment, etc.[3] Many hazardous dyes, namely, Rhodamine B (RhB), Methyl orange (MO), and Methyl violet (MV), are released

*For correspondence

Electronic supplementary material: The online version of this article (https://doi.org/10.1007/s12039-019-1700-z) contains supplementary material, which is available to authorized users.

Published online: 20 December 2019

into the water bodies by the dye industry without any treatment. These dyes have adverse effects on the environment and the ecosystem. RhB is carcinogenic and mutagenic, whereas high concentrations of MV can cause hypertension, fever, confusion, staining of skin, decolouration of urine, etc.[4] Although the conventional polysaccharide hydrogels are renewable, biodegradable, eco-friendly and non-toxic, but the vital problem lies in their low thermal and mechanical properties that limit their use in various applications such as tissue engineering, adsorbent, drug delivery, etc. Thus, the future development of polysaccharide hydrogels relies upon designing the stable hydrogel networks by crosslinking different polymers using various chemical and physical cross-linkages among the reactive functionalities present on polymeric chains.[5,6] In most of its applications, CMC was cross-linked either with itself or with other polymer chains to form a three-dimensional polymeric hydrophilic network, which was able to absorb large amount of water.[7,8] Gelatin, an ionic hydrophilic linear polypeptide with the $–NH_2$ and –COOH functionalities can improve the network structure and enhance the gel strength, hydrophilicity and functional properties of the hydrogels.[9–11] Dialdehyde carboxymethyl cellulose (DCMC), an oxidized polysaccharide can be synthesized via periodate oxidation of CMC, which is an extremely specific reaction to transform vicinal dihydroxyl (glycol) groups to paired aldehyde groups without significant side products.[12] This oxidation reaction involves specific cleavage of C_2-C_3 bond of the 1,4-glucan unit of CMC. The degree of oxidation of CMC could be manipulated by controlling the different reaction parameters such as the amount of periodate, temperature, time and presence of metal salts.[12] Furthermore, the dialdehyde polysaccharide can be cross-linked covalently with amino groups of gelatin by the Schiff base reaction to form a cross-linked hydrogel.[13–15] The strengthening of intramolecular and intermolecular structures *via* crosslinking is prerequisite to utilize these hydrogels in aqueous solutions as well as in biological systems. The cross-linking of DCMC and gelatin without using any extraneous cross-linker might result into a biopolymer-based hydrogel with better stability.[16] Herein, we report the development of a novel hydrogel synthesized by cross-linking DCMC and gelatin using the Schiff base reaction without employing any extraneous cross-linker and its utilization in the removal of Rhodamine B (RhB) and Methyl violet (MV). The maximum percentage of RhB and MV removed from the respective dye solutions using DCMC-cl-G hydrogel was 96.5% and 90% at pH 6.0, respectively.

2. Experimental

2.1 *Materials and physical measurements*

CMC sodium salt (degree of substitution (DS) = 0.7, average molar mass (Mw) = 250 kDa and viscosity 250–350 cps for 2% solution at 20 °C), gelatin (gel strength: 225 g Bloom, type B from bovine skin), sodium periodate, sodium hydroxide, ethanol, Rhodamine-B (RhB), methyl violet (MV) were obtained from Loba Chemie. All reagents used were of analytical grade and solutions were prepared using distilled water.

FTIR spectrum of a sample was recorded on Bruker Alpha FTIR spectrometer in the solid-state as a KBr pellet.

Morphological variations were studied using a high-resolution SEM (JEOL S150A). The dry sample was spread on a double-sided conducting adhesive tape, pasted on a metallic stub, coated with gold in anion sputter coating unit and was observed under JEOL-JXA-840A Electron probe microanalyzer at 20 kV.

Compressive properties were measured using a compression testing machine (100 Series Electromechanical Universal Test Machine, Test resources) at a strain rate of 0.2 mm/min up to 60% strain. Dynamic rheological measurements of the hydrogels were carried out with a rheometer (RheolabQC, Anton Paar, Austria) at 25 °C, using a parallel plate system, with a diameter of 50 mm and gap of 1 mm. Before the rheological measurements, hydrogels were equilibrated in the water at room temperature for two days.

Thermal studies were done from 50 °C to 700 °C at a heating rate of 10 °C per min using TGA/DTA 6300, SII EXSTAR 6000, INKARP instruments.

X-ray diffraction (XRD) measurements were carried out on an Empyrean Malvern Pan analytical diffractometer operating at 40 kV and 30 mA at a scan rate of 0.388 min^{-1} using parallel beam geometry and Cu-Kα radiation.

UV–Visible absorption spectra were measured using Shimadzu-1800 spectrophotometer in the solution state.

2.2 *Synthesis of dialdehyde of CMC*

In a Round Bottom Flask (RBF), CMC (1 g) and sodium periodate ($NaIO_4$) (1.51 g) were dissolved in 20 mL of distilled water and the pH of the solution was adjusted to 7.0 by the drop-wise addition of 0.5 M sodium hydroxide. After stirring the reaction mixture in dark for 72 h, the oxidized product was precipitated by pouring it into ethanol. The resultant precipitate was filtered out and dried at 40 °C till a constant weight was achieved for subsequent use.

2.3 *Determination of aldehyde content of DCMC*

The degree of oxidation of CMC was evaluated by determining the aldehyde content (AC) of DCMC using the rapid quantitative alkali consumption method.[17] The percentage of dialdehyde units was given by the following equation[17]:

$$\mathrm{AC}\,(\%) = \frac{\mathrm{v_1c_1} - 2\mathrm{v_2c_2}}{\mathrm{w}/160 \times 1000} \times 100 \qquad (1)$$

where, c_1 and c_2 (mol/L) represent the normality of NaOH and H_2SO_4, respectively; v_1 and v_2 (mL) represent the total volume of NaOH and H_2SO_4, respectively; w is the dry weight (g) of the DCMC sample, 160 is the average molecular weight of the repeating unit in DCMC.

2.4 *Synthesis of DCMC-cl-G hydrogel*

The solution of gelatin (1 g in 15 mL of water) was slowly added into DCMC suspension (15 mL, 1 g). The mixture obtained was sonicated to remove air bubbles and was kept at 40 °C with slow stirring for 2 h. The synthesized hydrogel was washed with water and then dried in a hot air oven at 50 °C to obtain a constant weight. The synthesized hydrogel was labelled as DCMC-cl-G.

2.5 *Swelling studies of hydrogels*

The swelling ratio of the hydrogels in the ultrapure water at ambient temperature was measured by the gravimetric method.[18] Dried hydrogels were weighed and equilibrated in double distilled water at 37 °C in an incubator till the attainment of constant weight. The equilibrium Swelling Ratio (SR) of the hydrogel was determined using the following equation[18]:

$$\text{Swelling Ratio (SR)} = \frac{(wt - wo)}{wo}\ \text{g/g} \qquad (2)$$

where w_t is the weight of the swollen gel after equilibrium at 37 °C and w_o is the weight of the dry gel.

The Ninhydrin assay was used to determine the cross-linking degree (%) or the amount of free amino groups present in the sample. The sample was weighed and heated with a Ninhydrin solution (2% w/w) at 100 °C for 20 min. After the test solution was cooled to room temperature and diluted in 95% ethanol, the optical absorbance of the solution was recorded with a UV-visible spectrophotometer (Shimadzu-1800) at 570 nm. The gelatin was used as control. The number of free amino groups measured in the sample was proportional to optical absorbance. The amount of free amino groups in gelatin (c_i) and in hydrogel (c_f) is proportional to the optical absorbance of the solution. The degree of cross-linking was calculated by the following equation:

$$\text{Cross-linking degree}\,(\%) = \frac{c_i - c_f}{c_f} \times 100.$$

2.6 *Adsorption of dyes*

2.6a *Preparation of stock solution of dyes*: For dye adsorption studies, stock solutions of MV and RhB were prepared by dissolving appropriate amounts of dyes in double-distilled water. The desired dyes concentrations (100 mg/L) were obtained by diluting the stock solutions.

2.6b *Adsorption of dyes onto the hydrogel*: The adsorption capacity of the hydrogel was studied by mixing dye solution (100 mL) with desired mass of hydrogel in 250 mL glass bottles and agitated on shaker until equilibrium was reached. After this, the dye loaded hydrogel was filtered from the solution and the concentration of dye in the solution before and after the adsorption was determined using a UV–Vis spectrophotometer (Shimadzu-1800) with λ 420 nm and 554 nm for MV and RhB, respectively. The optimum amount of hydrogel required for decolourization of dye was determined by varying its dose between 0.1–0.5 g. Further, adsorption experiments were performed by adjusting pH of dye solutions between 2 and 12 for an optimized hydrogel dose. The percentage removal of dye was obtained from the initial concentration of dye (c_o) and Equilibrium concentration of dye (c_e) in mg/L using the following equation,

$$\%\,\text{removal} = \frac{(c_o - c_e)}{c_e} \times 100. \qquad (3)$$

2.6c *Adsorption isotherm studies*: Adsorption isotherm studies were done to understand the adsorption mechanism. For these studies, initial dye concentration was varied in the range of 50–350 mg/L. The optimized dose of hydrogel was added to dye solutions of different concentrations and adsorption experiments were carried out using the above-mentioned procedure. The amount of dye uptake by hydrogel (q_e) in mg/g was calculated using the following equation

$$q_e = \frac{(c_o - c_e)}{m} \times V \qquad (4)$$

Where V is the volume (L) of dye and m is the mass (g) of hydrogel adsorbent

2.6d *Adsorption kinetics studies*: Kinetic studies of adsorption were carried-out by adding the optimized dose of hydrogel to 100 mL of dye solution (100 mg/L) and the mixture was stirred at 120 rpm and 35 °C. The amount of dye adsorbed at a particular time (q_t) was calculated using the following expression:

$$q_t\,(mg/g) = \frac{(c_o - c_t)}{m} \times V \quad (5)$$

where c_t is the concentration of dye at a particular time.

2.7 *Desorption studies*

The reusability of hydrogel after dye adsorption was investigated with five repeated cycles of adsorption and desorption. For this study, 0.2 g of hydrogel was added to 50 mL RhB solution (180 mg/L) at room temperature, pH 6 and agitated for 120 min to achieve the optimum adsorption. In a similar way, 0.3 g hydrogel was added to 50 mL MV solution (125 mg/L) at room temperature, pH 6 and agitated for 140 min. The dye loaded hydrogels were washed with distilled water, dried and recycled using 0.1 M HCl. The recycled hydrogel was used for the next adsorption cycle. The amount of RhB and MV during each adsorption-desorption cycle was determined using UV-Visible absorption intensity at λ_{max} of dyes. After each cycle, the binding sites of the adsorbent were regenerated using 50 mL of 0.1 M NaOH.

2.8 *Biodegradation studies*

The biodegradability of DCMC-cl-G hydrogel was studied using soil composting method.[19] Hydrogel samples were degraded in microbe-rich soil compost under controlled moisture conditions. The progress of degradation was evaluated by examining changes in weight, morphology (using SEM) and chemical composition (using FTIR spectroscopy) of hydrogel samples for twelve weeks.

3. Results and Discussion

3.1 *Synthesis*

Although hydrogels of CMC prepared via chemical cross-linking have been found to exhibit high swelling ratio due to electrostatic charges present on the network but it generally lacks mechanical strength.[20] The stabilization of hydrogels in an aqueous solution can be enhanced by cross-linking CMC with another compatible biopolymer *via* chemical and physical cross-linkages. In the present study, periodate oxidation of CMC was done to introduce a large number of aldehyde groups (Scheme S1, Supplementary Information). Its number was determined using quantitative alkali consumption method.[17] The aldehyde content (AC) for DCMC was estimated to be 60 ± 2%. Consequently, the synthesized DCMC was cross-linked to gelatin via the Schiff base reaction between aldehyde group of DCMC and primary amine groups of gelatin to form a hydrogel (Scheme 1). The hydrogel obtained is shown in Figure S1 (Supplementary Information) and its schematic drawing is presented in Figure 1 (see Section 3.3 for the basis of it). In the synthesised hydrogel, the chemical cross-linking between DCMC and gelatin, as well as the physical crosslinks among gelatin chains (hydrogen bonding due to α-helical conformation of gelatin) resulted in the formation of a three-dimensional network.[14]

3.2 *Swelling studies*

The hydrogel swells in an aqueous medium due to absorption of water owing to various van der Waals interactions among water and the different hydrophilic functional groups present on the hydrogel backbone. The swelling of a hydrogel is a result of diffusion of water into polymeric hydrogel network which causes expansion of polymeric network counterbalanced by elastic retractive forces.[21] Further, the degree of crosslinking among the different polymer chains can influence swelling behaviour of hydrogels. The crosslinking degree (%) was evaluated by the Ninhydrin assay. The chemical cross-linking between DCMC and gelatin *via* Schiff base reaction utilizes the free amino groups of the gelatin, thereby reducing the free amino groups in hydrogel. Ninhydrin reacts with free amino groups and produces a visible purple colour, detectable at 570 nm. The cross-linking degree of hydrogel was estimated as 50.31 ± 2.65 by the Ninhydrin assay.[22]

The water uptake capacity of hydrogel was analysed by its equilibrium swelling in distilled water at 37 °C. The swelling capacity of hydrogel was optimized with respect to pH, immersion time, and temperature. As shown in Figure 2a, the swelling capacity of the hydrogel was more at higher and lower pH values. At lower pH, most of the –COOH groups on DCMC backbone remained unionized, whereas, free $–NH_2$ groups on gelatin (crosslinking degree 50%) gets protonated and converted to $–NH_3^+$. The electrostatic repulsions among $–NH_3^+$ groups expand the network structure of hydrogel and increase its swelling capacity. Similarly, at higher pH, $–NH_3^+$ groups get deprotonated to $–NH_2$, and –COOH groups ionized to $–COO^-$. The interionic repulsions among $–COO^-$ groups increases the free volume, and in turn enhances the water inflow into hydrogel matrix. At pH values ranging from 4.0 to 6.0, –COOH and $–NH_2$ groups mostly remained unchanged or neutral, thereby decreasing repulsions and consequently the swelling ratio.

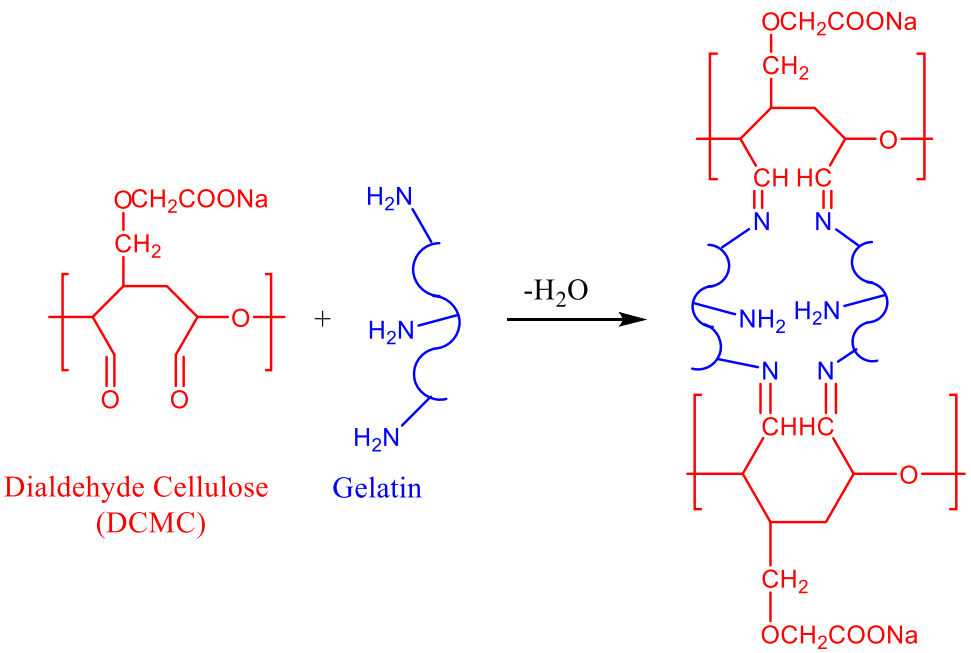

Scheme 1. Synthesis of DCMC-cl-G from DCMC and Gelatin *via* the Schiff base reaction.

As it is clearly evident from Figure 2b, the swelling ratio of hydrogel increased with increase in contact time. The maximum value of equilibrium swelling ratio at 37 °C was 74 g/g at pH 10.0 after 3 h. The swelling ratio of hydrogel increased with increase in temperature as shown in Figure 2b which might be due to enhanced mobility of polymer chains and decreased the cross-linked density of the matrix with increasing temperature. In 2016 Defu Li *et al.,* reported the equilibrium swelling ratio of the DCMC cross-linked gelatin-PEG hydrogel between 89 and 93%.[23] In the present study, the equilibrium swelling ratio was found to be 98.64% for DCMC-cl-G hydrogel.

3.3 *Spectroscopic characterization*

The FTIR spectra of all three samples were recorded in its solid state as shown in Figure S2 (Supplementary Information). The FTIR spectrum of DCMC showed characteristic absorption at 3400 cm^{-1} for O-H stretching vibration and at 1735 cm^{-1} for C=O stretching vibration of aldehyde group. The peak around 2900 cm^{-1} resulted from the stretching vibrations of $–CH_2$ groups. The peaks around 1423 cm^{-1} and 1603 cm^{-1} correspond to stretching vibration of $-COO^-$ groups. The bands near 1000 cm^{-1} were assigned to C-O-C stretching vibrations of carboxymethyl group of DCMC.

Gelatin showed characteristic absorption band at 3275 cm^{-1} (N-H stretching), 1629 cm^{-1} (amide-I), 1534 cm^{-1} (amide-II), 1239 cm^{-1} (amide-III) and symmetric stretching of $–COO^-$ groups at 1448 cm^{-1}. Amide-I represented C=O stretching/hydrogen bonding couple with COO, Amide-II represented the coupling of bending vibration of N-H groups and stretching vibrations of C-N groups, Amide-III is related to the vibrations in plane of C-N and N-H groups of bound amide.

The FTIR spectrum of DCMC-cl-G showed characteristic bands of DCMC cross-linked to gelatin by the Schiff base reaction. It displayed a broad band corresponding to the stretching frequency of –OH group in the region of 3300–3600 cm^{-1}, $-CH_2$ stretching vibration at 2916 cm^{-1}, symmetric stretching at 1163 cm^{-1} for C-C, C-O and C=N stretching vibration at 1629 cm^{-1}, C=O stretching vibration of the carboxylic group at 1706 cm^{-1}. The absorption of C=O stretching vibration of the aldehyde group at 1735 cm^{-1} disappeared due to its involvement in the Schiff base reaction with gelatin.[23] This confirms that all aldehyde groups are consumed to form the imine groups. Thus, the connectivity between the DCMC and gelatin allows us to construct the structure of DCMC-cl-G as shown in Figure 1.

3.4 *Scanning electron microscopy (SEM)*

The surface morphology of DCMC, gelatin, DCMC-cl-G hydrogel is shown in Figure 3. It is clearly indicating needle-like morphology of DCMC and

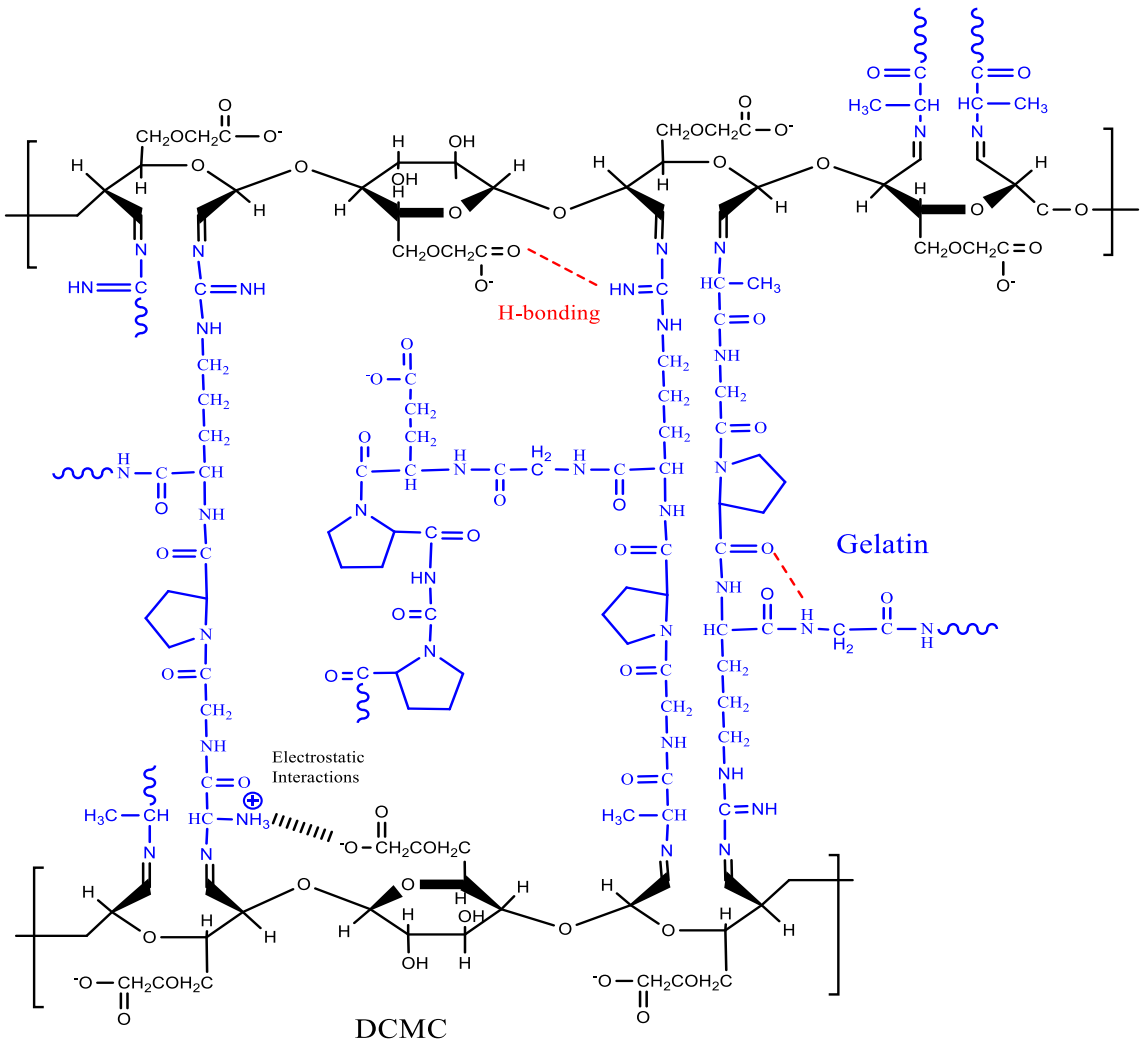

Figure 1. Schematic diagram of a cross-linked DCMC-cl-G hydrogel.

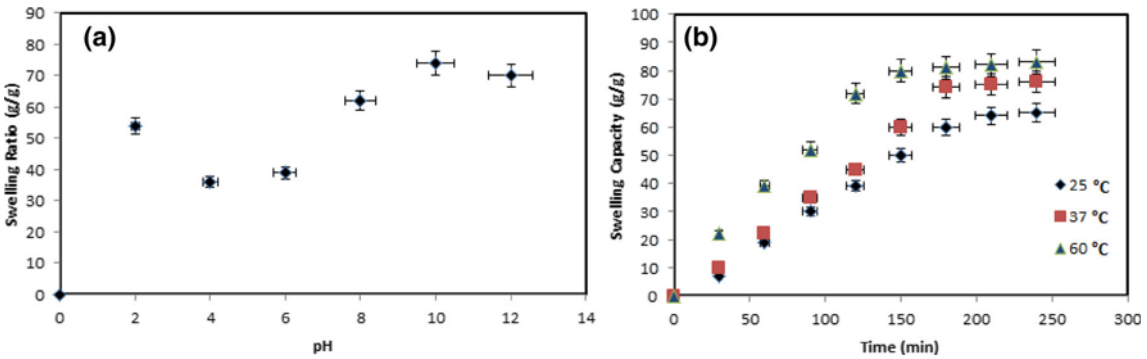

Figure 2. (a) Swelling kinetics of DCMC-cl-G hydrogel at different pH values and (b) swelling capacity of DCMC-cl-G hydrogel with temperature and time.

continuous phase of gelatin, respectively whereas the crosslinking of DCMC with gelatin resulted in an interconnected molecular network structure.[15] The hydrogel structure was rough, porous and more complex in comparison to the starting materials due to the formation of cross-linked network structure.

3.5 *Mechanical properties/rheological behaviour*

The purpose of synthesizing a hybrid hydrogel of DCMC and gelatin *via* the Schiff base reaction was to enhance its mechanical strength. Zeng *et al.* (2016) reported the synthesis of hydrogel with exceptional

mechanical strength by covalently crosslinking dialdehyde of micro fibrillated cellulose with gelatin.[15] The mechanical strength of hydrogel was determined by measuring its compressive strength. The compressive strength of hydrogel depends upon its composition, crosslinking degree and reaction conditions during its synthesis.[24] The compressive strength of DCMC-cl-G hydrogel was found to be 55 ± 0.76 kPa at 60% strain as shown in Figure 4a. It has been reported that the gelatin adds to elastic behaviour and gel strength of hydrogel.[25a] Here, the compressive strength was found to be higher in comparison to the previous results reported by Rajalaxmi Das *et al.* (2013) where gelatin hydrogels were cross-linked by cellulose nanowhiskers.[14] Figure 4b represents the storage modulus and loss modulus of the gel dependent upon angular frequency at a constant strain (1%) at room temperature. The storage modulus measures the elastic response of a material, whereas the loss modulus measures the viscous response. Both the storage modulus and loss modulus remained unchanged with increasing angular frequency, represents the well-cross-linked hydrogel with good mechanical strength. The storage modulus was always higher than the loss modulus over the observed frequency range. This indicates the typical polymer/gel behaviour displaying good elastic response.[25b]

3.6 *Thermal behaviour*

The thermograms of DCMC and DCMC-cl-G hydrogel are presented in Figure 5. The weight loss observed at initial stages was due to loss of moisture and volatile matter, while the weight loss at the later stages corresponded to the decomposition of the polymeric network. DCMC displayed initial weight loss of 7% due to removal of water up to 249.8 °C, followed by two-step weight loss of 55.1% and 86.8% at 250–372.8 °C and 455.8–577.8 °C, respectively. The hydrogel showed the initial weight loss of about 13% up to 210 °C due to removal of absorbed moisture and volatile molecules. It was followed by two-step weight loss of about 43.5% and 77.9% at 333.8–459.8 °C and 496.8–664.8 °C, respectively. It can be observed from thermograms that the DCMC started to decompose at 250 °C, whereas hydrogel initiated decomposition at 333.8 °C. As visible from Figure 5, the hybrid hydrogel was found to be thermally more stable in comparison to DCMC. The formation of three-dimensional cross-linked network

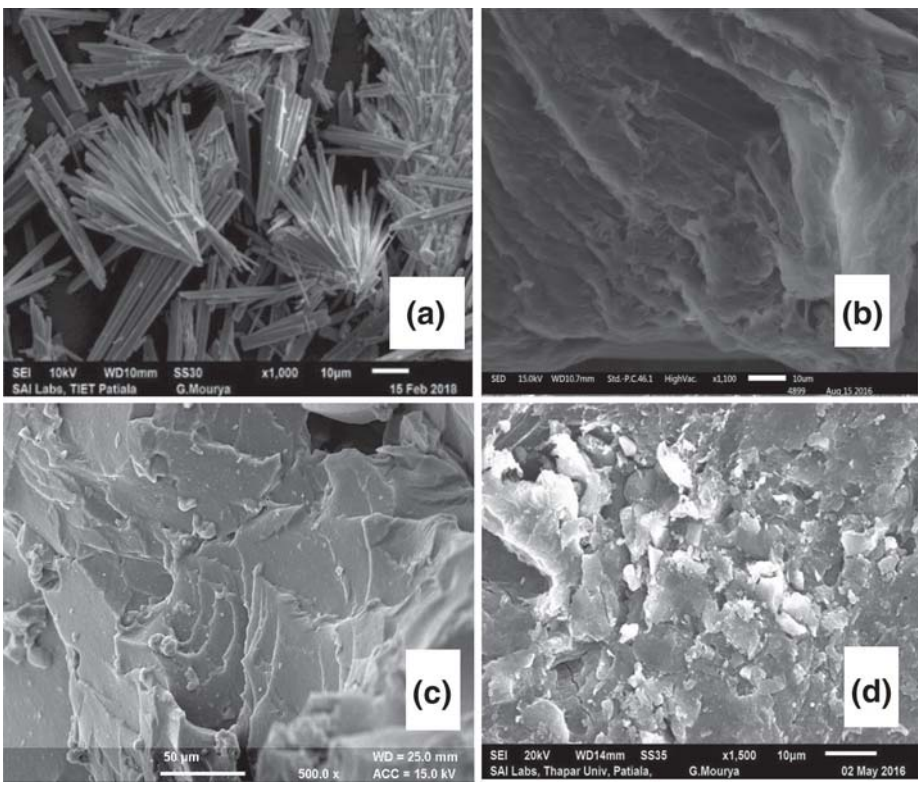

Figure 3. SEM images of (a) DCMC; (b) Gelatin; (c and d) DCMC-cl-G hydrogel.

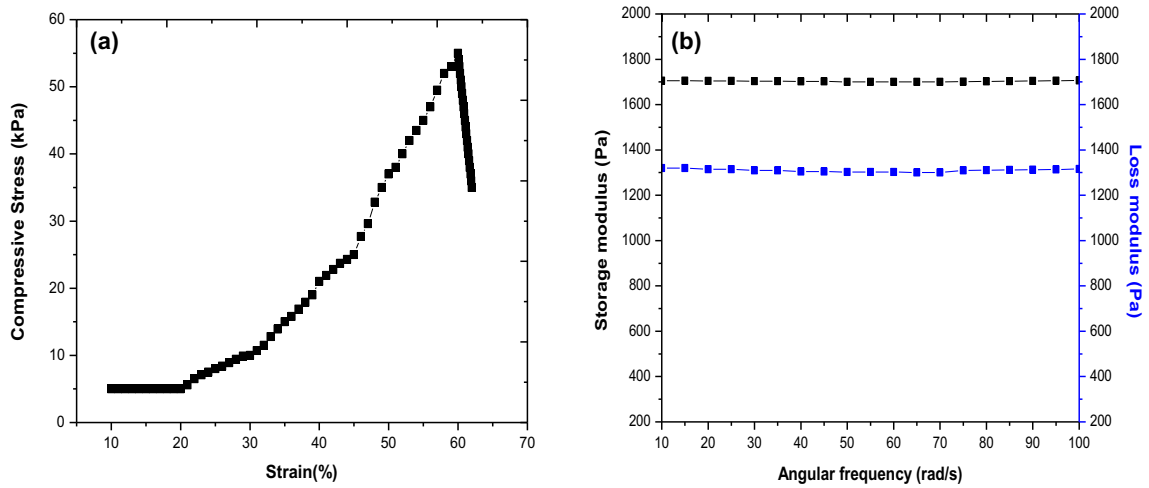

Figure 4. (a) Compressive strength of DCMC-cl-G hydrogel and (b) Storage modulus and loss modulus of the gel at a constant strain (1%).

structure because of chemical crosslinking between DCMC and gelatin led to high thermal stability of the synthesized hydrogel.[14]

3.7 *Powder X-ray diffraction (XRD) analysis*

The XRD patterns of CMC, DCMC, gelatin and DCMC-cl-G hydrogel are shown in Figure S3 (Supplementary Information). The XRD profile of CMC displayed a sharp peak at $2\theta = 20.25°$ indicating its typical semi-crystalline nature,[13a] whereas the pure gelatin exhibited a broad diffraction peak at $2\theta = 23.665°$ that showed its amorphous nature.[13a] Further, the XRD pattern of DCMC showed major sharp peaks at 2θ of 13.8, 16.2, 23.4, 26.9, 29.0, 30.6, 31.4, 34.0, reveals its crystalline nature compared to CMC.[13b] The hydrogel displayed a broad peak at $2\theta = 22°$. It indicates that the Schiff base reaction between DCMC and gelatin system decreased the crystallinity of DCMC due to destruction of long- or short-range regular patterns of polymeric chains.

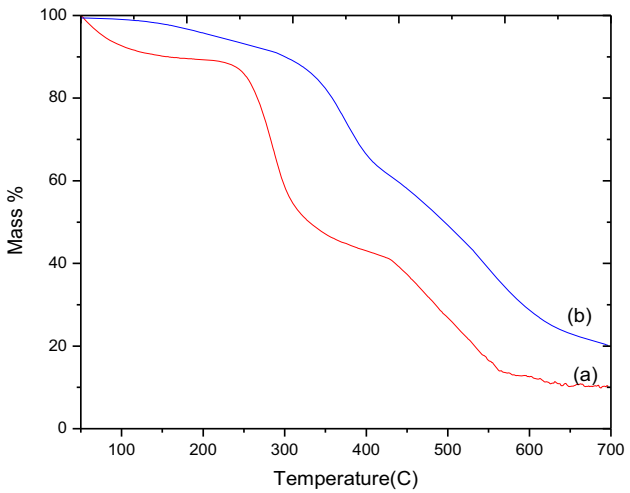

Figure 5. Thermograms of (a) DCMC and (b) DCMC-cl-G.

3.8 *Dye adsorption studies*

The treatment and removal of organic dyes from the textile effluents are one of the challenges faced by the environmentalists and industries. A vital requirement for the removal of dyes present from wastewater is to develop a cost-effective and highly efficient method. Low-cost polysaccharide-based hydrogels with high adsorption capacity, biocompatibility, and biodegradability can be considered as good candidates for adsorption of dyes from wastewater.[26] In the present study, DCMC-cl-G hydrogel was utilized as an adsorbent for the removal of cationic organic dyes i.e., Rhodamine B (RhB) and Methyl violet (MV) from water. The calculated 50% crosslinking degree between DCMC and gelatin *via* Schiff base reaction indicates that the remaining 50% functional groups on the polymer chains which includes carboxyl, hydroxyl and amine are free to interact with the chosen organic dyes.

3.8a *Effect of pH on dye adsorption*: The ionization and polarization of various functional groups present on the hydrogel backbone (carboxyl, hydroxyl, amine, amide and aldehyde) change with a change in pH of the solution. Thus, the effect of solution pH on the adsorption of RhB and MV dyes was studied as shown in Figure 6. It was observed that initially at low pH the dye adsorption was low, which increases with increase

in pH of solution. Both of these cationic dyes contain free amine groups which can easily interact with the carboxylate groups present on the hydrogel. However, at low pH, most of the carboxylic groups of the hydrogel remain unionized or protonated. Hence there was no significant adsorption of dye at lower pH values. At low pH, the adsorption occurred by electrostatic interaction of hydroxyl groups (-OH) of hydrogel with the protonated amines of dye.

It can be viewed from Figure 7a that the maximum dye adsorption was observed at pH 6 for both RhB and MV dyes. At this pH, the carboxylate groups were ionized and could better interact with the cationic dyes, thus dye adsorption was higher. However, after that the dye adsorption decreased with increase in pH as the competition between sodium ions and the cationic dye will increase resulting in decreased adsorption of RhB and MV.[27] It has been observed that the adsorption of cationic dyes can be rapidly increased on the surface of the hydrogel because of Van der Waals force, hydrogen bonding and electrostatic interactions.[28] The presence of carboxylic acid group in the RhB gives advantage over MV as this more polar group increases the interaction of the dye with the hydrogel through hydrogen bonding and electrostatic interactions. At pH 6, the maximum percentage removal of RhB and MV was 96.5% and 90%, respectively.

3.8b *Effect of contact time on dye adsorption*: The adsorption of RhB and MV dye by DCMC-cl-G hydrogel was studied at different contact time till the adsorption reaches equilibrium value (Figure 7b). The dye adsorption occurred by electrostatic interactions among the functional group of hydrogel and dye molecules. At the beginning of adsorption, the rate of adsorption was higher due to the availability of functional groups on hydrogel for the interaction. As the adsorption continued, the functional groups of the fixed amount of hydrogel in the aqueous medium exhausted and thus the rate of adsorption decreased and finally reached a dynamic equilibrium with a maximum adsorption value. The average time for hydrogel to attain equilibrium with MV and RhB was 140 min and 120 min, respectively.

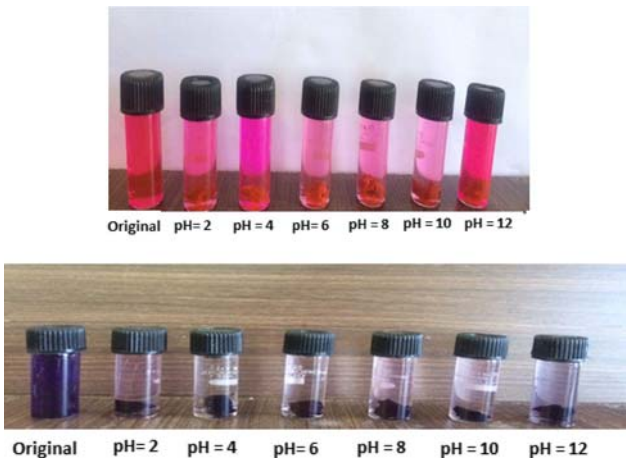

Figure 6. Effect of pH on RhB (top) and MV (bottom) dye adsorption by DCMC-cl-G at different pH values.

3.8c *Effect of hydrogel dose on dye adsorption*: The optimization of hydrogel dose required for effective removal of dyes from water was done by varying its amount between 0.1 and 0.5 g at pH 6.0 (Figure 7c). The maximum removal of RhB and MV was observed for hydrogel dosage of 0.2 g and 0.3 g, respectively. There was no significant change observed with an increasing amount of hydrogel. No doubt, more active sites would be available with an increased amount of hydrogel, however, an aggregation of a large number of hydrogel molecules might result in a decrease in the number of effective active sites available for interaction with dyes, and thereby do not affect its dye removal tendency.

3.8d *Adsorption isotherms*: The understanding and optimization of adsorption process including hydrogel's performance as an adsorbent. The study of adsorption mechanism and effective designing of the adsorption system can be done by applying commonly used isotherm models, such as Langmuir, Freundlich, Temkin and Dubinin-Radushkevish, Flory Huggins.[29] The details of these models are listed in Supplementary Information under Section S1. These models consider different types of adsorption site distributions according to the heat of adsorption profile as a function of the surface coverage. The adsorption isotherms evaluate the adsorption phenomenon at a constant temperature and pH. The overall adsorption behaviour can be predicted from the linear analysis of adsorption data using different isotherm models. Figure 8a shows the adsorption isotherms of RhB and MV dyes at 30 °C at an optimum pH 6.0. Initially, the dye adsorption by hydrogel was found to increase with increasing concentration of dye due to availability of adsorption sites over hydrogel, but on saturation of adsorption sites at higher concentrations of dyes led to the adsorption equilibrium and constant dye uptake (q_e) per unit mass of hydrogel.

Table 1 reports the calculated values of all adsorption constants along with the values of coefficients of determination (R^2) determined using the above-mentioned isotherms related to the adsorption of RhB and

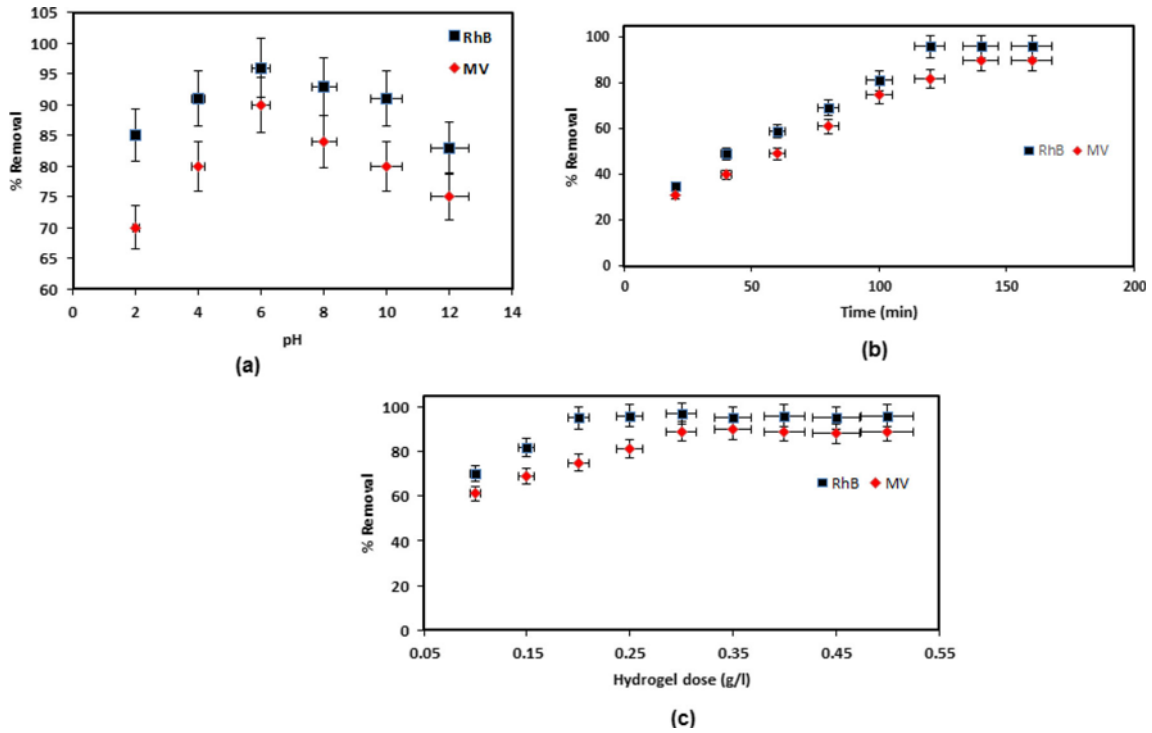

Figure 7. (a) Percentage removal of RhB and MV dyes, (b) effect of contact time on adsorption of RhB and MV at pH 6 and (c) effect of hydrogel dose on adsorption of RhB and MV.

MV dyes onto hydrogel. The maximum monolayer adsorption capacity of the hydrogel (q_m) obtained from Langmuir model was 763.4 mg/g for RhB and 584.7 mg/g for MV. The separation factor, R_L of the Langmuir model was much less than one which implies favourable adsorption for both the dyes. The value of 1/n obtained from Freundlich isotherm (0.288 for RhB and 0.318 for MV) indicates the favourable adsorption over the entire range of concentrations studied. The Temkin and D-R models were used to calculate heat of adsorption (β) and mean free energy of adsorption (E) of adsorption (Table 1). The heat of adsorption is usually larger for chemisorption as compared to physisorption. [30] The E and β values are found to be lower than 8 kJ mol^{-1} and 20 kJ mol^{-1}, respectively, which is an indication of physisorption.[31,32] The values of E and β mentioned in Table 1 indicates the adsorption of RhB and MV dyes over hydrogel as a case of physisorption. The negative values of ΔG° (−17.17 kJ mol^{-1} for RhB and −17.30 kJ mol^{-1} for MV) calculated from Flory-Huggins isotherm model supports a spontaneous adsorption process of exothermic nature. The value of R^2, the correlation coefficient, much higher and close to unity for Langmuir isotherm in comparison to other isotherms confirms the applicability of Langmuir model to the adsorption data related to adsorption of RhB and MV onto hydrogel (Table 1).

The maximum adsorption capacity of the synthesized hydrogel in the present study with the other polysaccharide hydrogels. The maximum adsorption capacity of RhB using DCMC-cl-G hydrogel as adsorbent (763.4 mg/g) was found to be comparable with hydrogel synthesized from gum ghatti and acrylic acid (819.67 mg/g).[32] The maximum adsorption capacity of MV using DCMC-cl-G hydrogel adsorbent (non-nanocomposite) was 584.7 mg/g, whereas it was around 642 mg/g with xanthan/Fe_3O_4 hydrogel,[33] which is a nanocomposite. Thus, more adsorption was expected, and about 340 mg/g with polyacrylamide grafted xanthan gum hydrogel containing nanosilica was far behind than the reported hydrogel in this present study.[34]

3.8e *Adsorption kinetics*: The process of adsorption involves adhesion of adsorbate molecules on the surface of the adsorbent. Adsorption kinetics extracts the adsorption rate constant from the time dependence of concentrations. Adsorption kinetics for the uptake of RhB and MV onto DCMC-cl-G hydrogel was investigated using pseudo-first-order and pseudo-second-order kinetics. The details of both the models are listed in Section S2 of the Supplementary Information. The effect of time and initial concentration of dyes on the adsorption of RhB and MV is represented in Figure 8b. The adsorption

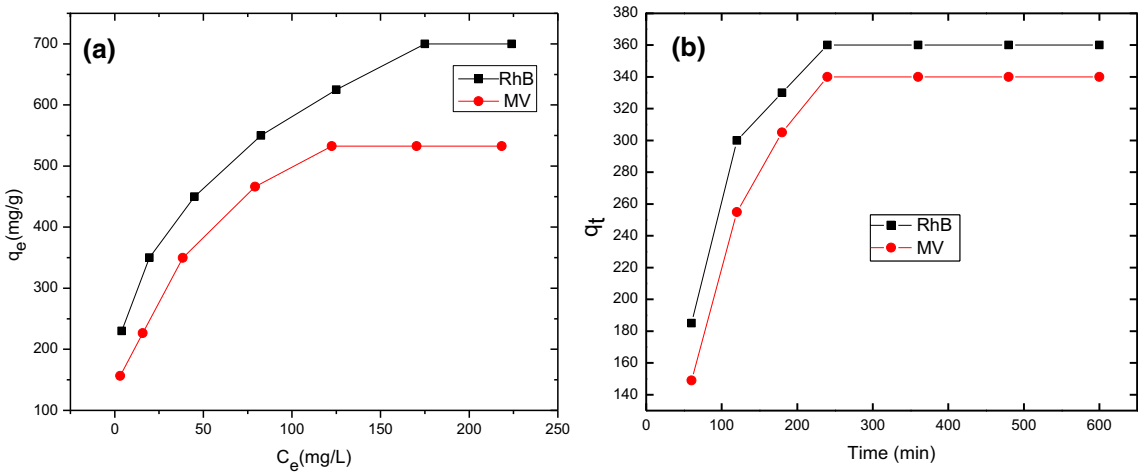

Figure 8. (a) Adsorption isotherms of RhB and MV dyes at 30 °C and pH 6.0 and (b) Effect of time and initial concentration of dyes on the adsorption of RhB and MV.

Table 1. Isotherm parameters for the adsorption of RhB and MV onto DCMC-cl-G hydrogel.

Isotherms	Isotherm constants	RhB	MV
Langmuir	q_m (mg/g)	763.4	584.7
	b	0.044	0.056
	R_L	0.061-0.311	0.048-0.263
	R^2	0.99125	0.99214
Freundlich	K_F	152.8	105.96
	1/n	0.288	0.318
	R^2	0.98488	0.96529
Temkin	β (J mol^{-1})	285.2	233.37
	K_T (L g^{-1})	1.074	1.0217
	R^2	0.95645	0.93814
Dubinin-Radushkevich (D-R)	$q_{s\ (mg/g)}$	464.5	593.6
	E (kJ mol^{-1})	1.334	1.367
	R^2	0.71248	0.74907
Flory-Huggins	K_{FH} (L mol^{-1})	1326.1	1236.9
	n	1.345	1.205
	ΔG° (kJ mol^{-1})	−17.17	−17.3
	R^2	0.95076	0.95749

equilibrium was approached within the same period of time for both the dyes i.e., 240 min. The data related to the kinetics of adsorption of RhB and MV onto DCMC-cl-G hydrogel was fitted using the above-mentioned kinetic models (Figures S4 and S5, Supplementary Information). The model parameters i.e., values of pseudo rate constants (k_1 and k_2) and equilibrium dye adsorption (q_e) along with the statistical parameters for these model fitting are given in Table 2.

On analysing the values of R^2 (coefficient of determination) for pseudo-first-order and pseudo-second-order kinetics (Table 2), it was observed that pseudo-second-order rate model better fits the kinetic data for adsorption of both RhB and MV onto DCMC-cl-G hydrogel. Further, the calculated and the experimental values of q_e in pseudo-second-order rate model were more consistent in comparison to the pseudo-first-order rate model. Hence, the adsorption of both RhB and MV onto DCMC-cl-G hydrogel can be better described using the pseudo-second-order kinetic model.

3.9 *Desorption studies*

The reusability of the hydrogel as dye adsorbent was studied with repeated cycles of adsorption-desorption. Cationic dyes were successfully desorbed from the hydrogel surface using 0.1 M HCl. The adsorption-

desorption efficiency was found to be near 100% in the first two cycles for both the dyes as shown in Figure 9. For the next cycle (third), there was a slight decrease in adsorption-desorption efficiency. After the fifth cycle, the adsorption-desorption capacity of hydrogel decreased by about 15% for both the dyes. The results indicate that the hydrogel synthesized in the present work can be utilized as a good recyclable adsorbent for cationic dyes.

3.10 *Biodegradation of DCMC-**cl-G** hydrogel*

Hydrogels based upon natural polymers have inherent tendency to degrade aerobically as well as anaerobically.[32] Though, in the present study, backbone, CMC was chemically modified to DCMC and further cross-linked to gelatin by C=N bonds to form three-dimensional hydrogel network. The chemical modification of natural polymers might affect its biodegradability. Here, the purpose of studying biodegradation of hydrogel was to ascertain its biodegradable nature. It was observed that the weight of hydrogel decreased (Table 3) continuously with time due to activity of microbes present in soil upon hydrogel (Figure S6, Supplementary Information). The maximum weight loss was recorded as 82.67% over duration of twelve weeks. The chemical changes in DCMC-cl-G hydrogel during its various stages of degradation was confirmed through FTIR analyses and the changes in morphology during different stages of degradation were studied by means of SEM.

3.11 *SEM studies after biodegradation*

The morphological analysis of DCMC-cl-G hydrogel before and after degradation was done using SEM (-Figure 10). Though the hydrogel surface was heterogeneous before subjecting to biodegradation, the intensity and number of cracks were comparatively less. The microorganisms present in the composting soil attacked and decomposed the cross-linked networks of hydrogel and continuously increased the discontinuities of the surface as visible from SEM images of hydrogel samples taken up to eight weeks. The degradation of the hydrogel sample takes place by breaking of cross-linkages and covalent bonds between the different polymer chains. Finally, the large number of holes and cracks broke down the bulk hydrogel to intermittent particles with polydisperse size distribution after the 12th week of biodegradation. The enzymatic and chemical degradation caused by microorganisms was responsible for the complete breakdown of the hydrogel network.[35]

Table 2. Kinetics parameters of adsorption of RhB and MV onto DCMC-cl-G hydrogel.

Model	RhB	MV
Pseudo 1st order		
$q_{e\ (mg/g)\ calculated}$	176.5	169
$q_{e\ (mg/g)\ experimental}$	373	354
k_1	0.045	0.056
R^2	0.96746	0.97979
Pseudo 2nd order		
$q_{e\ (mg/g)\ calculated}$	360	338
$q_{e\ (mg/g)\ experimental}$	373	354
k_2	0.54	0.974
R^2	0.99789	0.99851

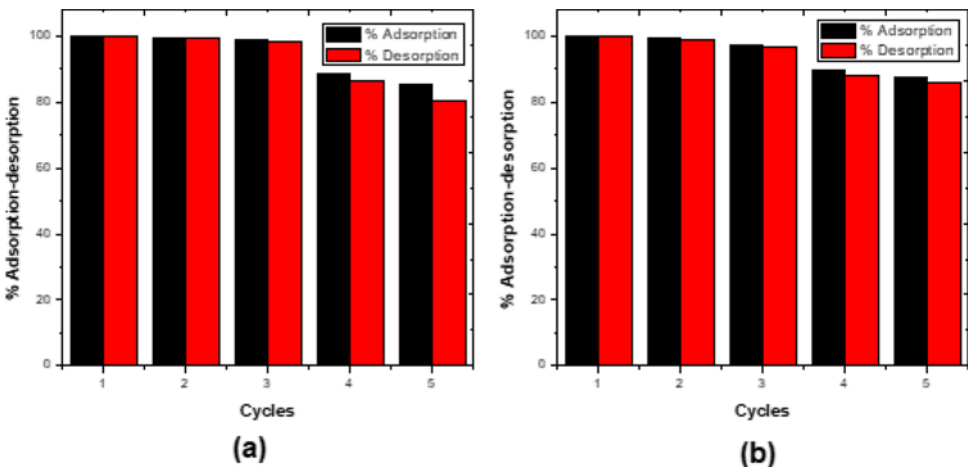

Figure 9. Performance of hydrogel for five cycles of adsorption-regeneration for (a) RhB and (b) MV.

Table 3. Weight loss of DCMC-cl-G hydrogel during degradation using soil composting method.

Weeks	% Weight loss
1	7.83
2	14.89
3	20.65
4	25.07
5	30.95
6	36.78
7	48.85
8	54.92
9	60.78
10	69.15
11	75.31
12	82.67

3.12 *FTIR studies*

The degradation of DCMC-cl-G under controlled conditions was further confirmed through the changes observed in FTIR spectra before and after degradation of the hydrogel sample for twelve weeks (Figure 11). The labelled FTIR spectrum for the biodegradation studies is shown in Figure S7, Supplementary Information. The FTIR spectrum of DCMC-cl-G displayed a broad band in the range of 3300–3500 cm^{-1} for O-H stretching vibration, -CH_2 stretching vibration at 2916 cm^{-1}, C-C and C-O symmetric stretching at 1163 cm^{-1}, C=N stretching vibration at 1629 cm^{-1} and C=O stretching vibration of aldehyde group at 1735 cm^{-1}. However, the degradation of hydrogel sample recorded in different weeks showed an increase in transmittance (or decreased absorbance) and shifting of some of the peaks in FTIR spectra. The changes in FTIR spectra were observed due to initial cleavage of cross-linked networks between different polymer chains and final cleavage of covalent bonds by the different microorganisms present in soil.[35] Peaks initially appearing at 1735 cm^{-1}, 1629 cm^{-1} and 1163 cm^{-1} exhibited variations in intensity as well as position. Thus, FTIR studies of DCMC-cl-G during different stages of degradation confirmed the biodegradability of the polymer sample in soil compost within a period of twelve weeks.

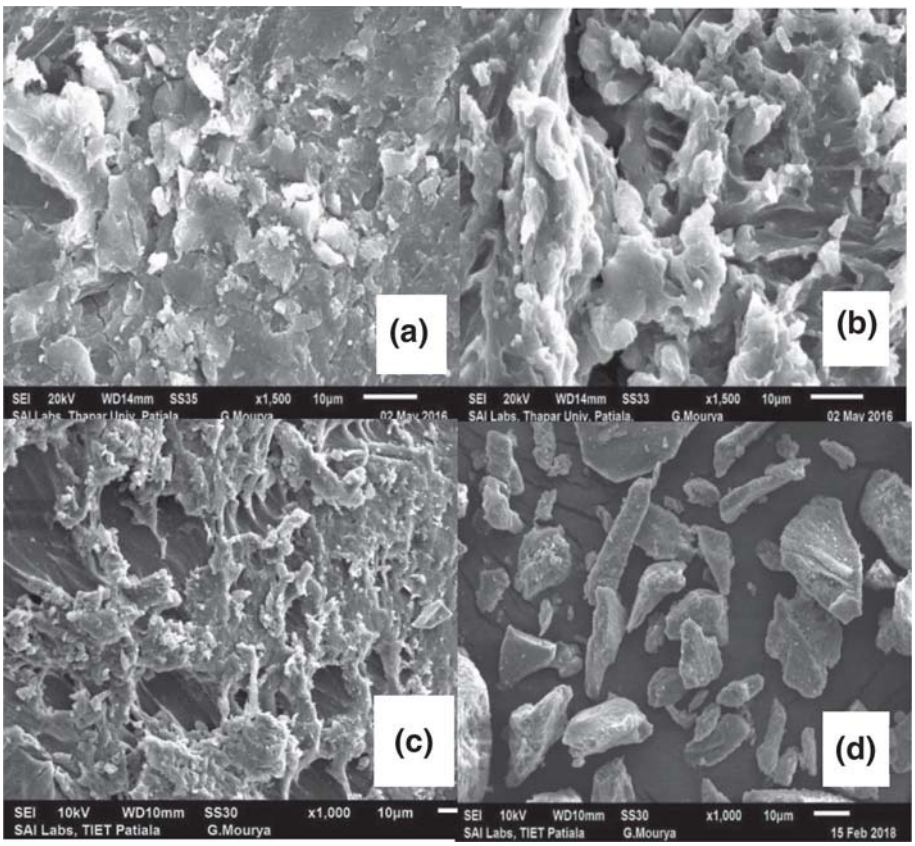

Figure 10. SEM images of DCMC-cl-G hydrogel during (a) 1st week, (b) 4th week, (c) 8th week, (d) 12th week of degradation.

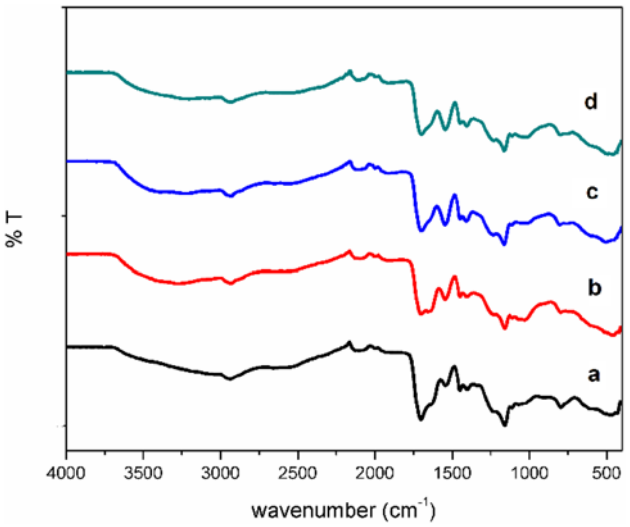

Figure 11. FTIR spectra of (a) DCMC-cl-G before degradation. (b) DCMC-cl-G after one-week degradation. (c) DCMC-cl-G after six weeks degradation. (d) DCMC-cl-G after twelve weeks degradation.

4. Conclusions

The novel hydrogel (DCMC-cl-G) was successfully synthesized *via* crosslinking of DCMC and gelatin using the Schiff base reaction. The hydrogel was found to be thermally as well as mechanically stable with a maximum swelling capacity of 74 g/g at pH 10.0 and 37 °C. Biodegradation studies confirmed 82.67% degradation of the hydrogel sample within a period of twelve weeks. Further, the hydrogel sample was successfully utilized as a bio adsorbent for the RhB and MV dyes in aqueous solution. The value of R^2 (the correlation coefficient) is much higher for Langmuir isotherm in comparison to other isotherms confirmed the applicability of the Langmuir model to adsorption of RhB and MV onto the hydrogel. The adsorption kinetic data of both RhB and MV dyes fitted well with the pseudo-second-order kinetic model rather than the pseudo-first-order rate model. The scope of this study is to add to the widespread applications of biopolymers as bio adsorbents with improved thermal and mechanical properties. Thus, this hydrogel with improved properties and good biodegradability could be successfully applied as a bio adsorbent in aqueous solutions as well as in biological systems.

Supplementary Information (SI)

As synthesized Hydrogel, FTIR and PXRD of gel and starting materials, Fit of kinetic data to pseudo-first-order model for the adsorption of RhB and MV, % weight loss of Hydrogel with time and labelled FTIR spectra for biodegradation studies are represented in Figures S1–S7. Details of isotherm and kinetic models are described in Sections S1 and S2. Supplementary Information is available at www.ias.ac.in/chemsci.

Acknowledgements

X-ray facility at Dr. B R Ambedkar is gratefully acknowledged.

References

1. (a) Akan J C, Abdulrahman F I, Ayodele J T and Ogugbuaja V 2009 Impact of Tannery and Textile Effluent on the Chemical Characteristics of Challawa River, Kano State, Nigeria *Aust. J. Basic Appl. Sci*. **3** 1933; (b) Lotfy S and Abou Taleb M F 2018 Free radical polymerization of polyvinyl butyral/polyethylene glycol diacrylate copolymer for removing organic dyes from waste water *Polym. Bull*. **75** 2865; and (c) Shah M P 2016 Industrial Wastewater Treatment: A Challenging Task in the Industrial Waste Management *Adv. Recycl. Waste Manage.: Open Access* **2** 115
2. Capar G, Yetis U and Yilmaz L 2006 Membrane based strategies for the pre-treatment of acid dye bath wastewaters *J. Hazard. Mater.* **135** 423; (b) Zahrim A Y, Tizaoui C and Hilal N 2011 Coagulation with polymers for nanofiltration pre-treatment of highly concentrated dyes: A review *Desalination* **266** 1; (c) Liu C H, Wu J S, Chiu H C, Suen S Y and Chu K H 2007 Removal of anionic reactive dyes from water using anion exchange membranes as adsorbers *Water Res.* **41** 1491; and (d) Sheshmani S, Ashori A, Hasanzadeh S 2014 Removal of Acid Orange 7 from aqueous solution using magnetic graphene/chitosan: A promising nano-adsorbent *Int. J. Biol. Macromol.* **68** 218
3. (a) Bhatia J K, Kaith B S and Kalia S 2013 Polysaccharide Hydrogels: Synthesis, Characterization, and Applications In: *Polysaccharide Based Graft Copolymers* (Berlin: Springer) Ch. 7 pp. 271–290; (b) Pathania D, Verma C, Negi P, Tyagi I, Asif M, Kumar N S, Al-Ghurabi E. H, Agarwal S and Gupta V K 2018 Novel nanohydrogel based on itaconic acid grafted tragacanth gum for controlled release of ampicillin *Carbohydr. Polym.* **196** 262; (c) Wang W B, Zhang H X, Shen J F and Ye M X 2018 Facile preparation of magnetic chitosan/poly (vinyl alcohol) hydrogel beads with excellent adsorption ability via freezing-thawing method *Colloid. Surf. A* **553** 672; (d) Sampath S, Choudhury N A and Shukla A K 2009 Hydrogel membrane electrolyte for electrochemical capacitors *J. Chem. Sci.* **121** 727
4. Vadivelan V and Kumar K V 2005 Equilibrium, kinetics, mechanism, and process design for the sorption of methylene blue onto rice husk *J. Colloid. Interf. Sci*. **286** 90
5. Liu S, Kang M, Li K, Yao F, Oderinde O, Fu G and Xu L 2018 Polysaccharide-templated preparation of mechanically-tough, conductive and self-healing hydrogels *Chem. Eng. J.* **334** 2222

6. Monier M, Abdel-Latif D A and Ji H F 2016 Synthesis and application of photo-active carboxymethyl cellulose derivatives *React. Funct. Polym.* **102** 137
7. Capanema N S V, Mansur A A P, deJesus A C, Carvalho S M, de Oliveira L C and Mansur H S 2018 Superabsorbent crosslinked carboxymethyl cellulose-PEG hydrogels for potential wound dressing applications *Int. J. Biol. Macromol.* **106** 1218
8. Benhalima T, Ferfera-Harrar H and Lerari D 2017 Optimization of carboxymethyl cellulose hydrogels beads generated by an anionic surfactant micelle templating for cationic dye uptake: Swelling, sorption and reusability studies *Int. J. Biol. Macromol.* **105** 1025
9. Cui L, Jia J, Guo Yi, Liu Y and Zhu P 2014 Preparation and characterization of IPN hydrogels composed of chitosan and gelatin cross-linked by genipin *Carbohyd. Polym*. **99** 31
10. Nieuwenhove I V, Salamon A, Petersb K, Graulusa G-J, Martinsc J C, Frankeld D, Kersemanse K, Vose F D, Vlierberghea S V and Dubruela P 2016 Gelatin- and starch-based hydrogels. Part A: Hydrogel Development, characterization and coating *Carbohyd. Polym.* **152** 129
11. Manna P J, Mitra T, Pramanik N, Kavith V, Gnanamani A and Kundu P P 2015 Potential use of curcumin loaded carboxymethylated guar gum grafted gelatin film for biomedical applications *Int. J. Biol. Macromol.* **75** 437
12. Li H, Wu B, Mu C and Lin W 2011 Concomitant degradation in periodate oxidation of carboxymethyl cellulose *Carbohyd. Polym.* **84** 881
13. (a) Balakrishnan B, Joshi N and Banerjee R 2013 Borate aided Schiff's base formation yields in situ gelling hydrogels for cartilage regeneration *J. Mater. Chem. B* **1** 5564; (b) EL-Sayed N S, El-Ziaty A K, El-Meligy G, Nagieb Z A 2017 Syntheses of New Antimicrobial Cellulose Materials Based 2-((2-aminoethyl)amino)-4-aryl-6-indolylnicotinonitriles *Egypt. J. Chem.* **60** 465
14. Dash R, Foston M and Ragauskas A J 2013 Improving the mechanical and thermal properties of gelatin hydrogels cross-linked by cellulose nanowhiskers *Carbohyd. Polym.* **91** 638
15. Zheng X, Zhang Q, Liu J, Pei Y and Tang K 2013 A unique high mechanical strength dialdehyde microfibrillated cellulose/gelatin composite hydrogel with a giant network structure *RSC Adv.* **6** 71999
16. Sethi S, Kaith B S, Saruchi, Kumar V 2019 Fabrication and characterization of microwave assisted carboxymethyl cellulose-gelatin silver nanoparticles imbibed hydrogel: Its evaluation as dye degradation *React. Funct. Polym.* **142** 134
17. Hofreiter B T, Alexander B H and Wolff I A 1955 Rapid Estimation of Dialdehyde Content of Periodate Oxystarch through Quantitative Alkali Consumption *Anal. Chem.* **27** 1930
18. Mandal B and Ray S K 2014 Swelling, diffusion, network parameters and adsorption properties of IPN hydrogel of chitosan and acrylic copolymer *Mater. Sci. Eng.* C **44** 132
19. Mittal H, Mishra S B, Mishra A K, Kaith B S, Jindal R and Kalia S 2013 Preparation of poly (acrylamide-co-acrylic acid)-grafted gum and its flocculation and biodegradation studies *Carbohyd. Polym.* **98** 397
20. Sannino A, Demitri C and Madaghiele M. 2009 Biodegradable Cellulose-based Hydrogels: Design and Applications *Materials* **2** 353
21. Guilherme M R, Aouada F A, Fajarado A R, Martins A F, Paulino A T, Davi M F T, Rubira A F and Muniz E C 2015 Superabsorbent hydrogels based on polysaccharides for application in agriculture as soil conditioner and nutrient carrier: A review *Eur. Polym. J.* **72** 365
22. Wu S C, Chang W H, Dong G C, Chen K Y, Chen Y S, Yao C H 2011 Cell adhesion and proliferation enhancement by gelatin nanofiber scaffolds *J. Bioact. Compat. Polym.* **26** 565
23. Li D, Ye Y, Li D, Li X and Mu C 2016 Biological properties of dialdehyde carboxymethyl cellulose crosslinked gelatin–PEG composite hydrogel fibers for wound dressings *Carbohyd. Polym.* **137** 508
24. Khorshidi S and Karkhaneh A 2016 A self-crosslinking tri-component hydrogel based on functionalized polysaccharides and gelatin for tissue engineering applications *Mater. Lett.* **164** 468
25. (a) Wang W-B, Huang D-J, Kang Y-R and Wang A-Q 2013 One-step in situ fabrication of a granular semi-IPN hydrogel based on chitosan and gelatin for fast and efficient adsorption of Cu^{2+} ion *Colloid. Surf. B: Biointerf.* **106** 51; (b) Tong Y, Zhang Y, Liu Y, Cai H, Zhang W and Tan W-S 2018 POSS-enhanced thermo sensitive hybrid hydrogels for cell adhesion and detachment *RSC Adv.* **8** 13813
26. Tu H, Yu Y, Chen J, Shi X, Zhou J, Deng H and Du Y 2017 Highly cost-effective and high-strength hydrogels as dye adsorbents from natural polymers: chitosan and cellulose *Polym. Chem.* **8** 2913
27. Zhu L, Guan C, Zhou B, Zhang Z, Yang R, Tang Y and Yang J 2017 Adsorption of Dyes onto Sodium Alginate Graft Poly(Acrylic Acid*co*-2-Acrylamide-2-Methyl Propane Sulfonic Acid)/ Kaolin Hydrogel Composite *Polym. Polym. Compos.* **25** 627
28. (a) Gong R, Ye J J, Dai W, Yan X Y, Hu J, Hu X, Li S and Huang H 2013 Adsorptive Removal of Methyl Orange and Methylene Blue from Aqueous Solution with Finger-Citron-Residue-Based Activated Carbon *Ind. Eng. Chem. Res.* **52** 14297; (b) Kumar N, Mittal H, Parashar V, Ray S S and Ngila J C 2016 Efficient removal of rhodamine 6G dye from aqueous solution using nickel sulphide incorporated polyacrylamide grafted gum karaya bionanocomposite hydrogel *RSC Adv.* **6** 21929
29. Mittal H, Maity A and Ray S S 2015 Effective removal of cationic dyes from aqueous solution using gum ghatti-based biodegradable hydrogel *Int. J. Biol. Macromol.* **79** 8
30. Dumeignil F, Paul J-F and Paul S 2017 Heterogeneous Catalysis with Renewed Attention: Principles, Theories, and Concepts *J. Chem. Edu.* **94** 675
31. Itodo A U and Itodo H U 2010 Sorption Energies Estimation Using Dubinin-Radushkevich and Temkin Adsorption Isotherms *Life Sci. J.* **7** 31
32. Fosso-Kankeu E, Mittal H, Mishra S B and Mishra A K 2015 Gum ghatti and acrylic acid based biodegradable

hydrogels for the effective adsorption of cationic dyes *J. Ind. Eng. Chem.* **22** 171
33. Mittal H, Kumar V, Saruchi and Ray S S 2016 Synthesis and flocculation properties of gum ghatti and poly(acrylamide-co-acrylonitrile) based biodegradable hydrogels *Int. J. Biol. Macromol.* **89** 1
34. Ghorai S, Sarkar A, Raoufi M, Panda A B, Schönherr H and Pal S 2016 Enhanced Removal of Methylene Blue and Methyl Violet Dyes from Aqueous Solution Using a Nanocomposite of Hydrolyzed Polyacrylamide Grafted Xanthan Gum and Incorporated Nanosilica *Appl. Mater. Interf.* **6** 4766
35. Mittal H, Jindal R, Kaith B S, Maity A and Ray S S 2014 Synthesis and flocculation properties of gum ghatti and poly(acrylamide-co-acrylonitrile) based biodegradable hydrogels *Carbohyd. Polym.* **114** 321